XL CILAMCE
IBERO-LATIN AMERICAN CONGRESS ON COMPUTATIONAL METHODS IN ENGINEERING
NOVEMBER 11-14, 2019
Praiamar Natal Hotel & Convention
Natal, RN-BRAZIL

A POSITIONAL FINITE ELEMENT FORMULATION FOR TENSION STRUCTURES ANALYSIS

Adriana P. de O. Silva
Humberto B. Coda
adriana.oliveiras@usp.br
hbcoda@sc.usp.br
School of Engineering of São Carlos of the University of São Paulo
Av. Trab. São Carlense, 400, 13566-590, São Paulo, Brazil

Abstract. This paper presents a total Lagrangian formulation of the Finite Element Method (FEM) and its implementation, for static and dynamic analysis of tension structures. The proposed formulation is based on the Principle of the Minimum Mechanical Energy written regarding nodal positions, not displacements. The adopted finite elements are truss elements, which are adapted to simulate positional actuators (active elements). Using these active elements one can simulate pre-tensioned cables and compressive actuators. It is also possible to adjust tension in the cables in order to guarantee its continuity for different spans of general suspension or tension structures. The resulting nonlinear system of equations is iteratively solved using the Newton-Raphson method. The classical Newmark equations are used to integrate time and three techniques to eliminate the numerical singularity of unstressed cable problems are employed. The linear elastic constitutive law of Saint-Venant-Kirchhoff is considered, which relates second Piola-Kirchhoff stress and Green-Lagrange strain, but any other constitutive model can be used. Representative examples are presented to validate the proposed formulation.

Keywords: Finite element method, Positional formulation, Tension structures, Truss element, Cable

1 Introduction

Structures in cables have a noble use in civil engineering, resulting in lightweight and elegant structures, with interesting applications where large spaces are needed, as bridges, stadiums, bus stations and airports, among others. Different structural cable arrangements are possible, which for cable roof the most usual are: simply suspended cables, pretensioned cable beams, pretensioned cable nets, tensioned straight cables and tensegric shells, as described by Santoso [1] and Buchholdt [2]. In addition, there are basically two distinct configurations for cable-supported bridges, which are the suspension bridges and the cable-stayed bridges.

Structural analysis of cable structures, given analytically, is quite complicated, since they are structures with high degree of nonlinearity, mainly in assembly phase and when subjected to dynamic actions. Due to the characteristics of this system, to define a configuration and a proper tension on each cable element without overloading certain cables, is the challenge associated with the design of cable structures.

There are some current scientific papers denoting strategies for calculating an isolated cable or structures composed of cables, some of them used analytical methods and also iterative methods to implement it, such as Jia et al. [3], Jung, Min and Kim [4], Wang, Chai and Xu [5] and Zhang et al. [6] to analyze statically a suspension bridge, as well done by Chen et al. [7] to analyze cable-stayed bridges.

Several numerical analyses, that as well-known, is a way to converting a continuous problem to a discrete problem, have been published in this context, mainly using the Finite Element Method (FEM), as done by El Debs [8]; Chatzis and Deodatis [9]; Filho [10]; Feng et al. [11] and Kim, Lee and Chang [12], the last also uses a force based shape-finding analysis of a suspension bridge. Cardoso [13] also used FEM, written in terms of nodal positions, as one of the models to analyze an isolated cable.

Regarding numerical modeling one can see, for example, in Ytza [14] a numerical modeling of cable-stayed bridges to find a method to obtain a good load distribution in the cables, or Feng, Shen and Wang [15] that studied the thermal stress and crack propagation due to temperature on the cable-stayed bridge pylon. In the same field of thermal analysis, but as an experimental study, as done by Yang et al. [16].

Moreover, many papers concerning the optimization of cable structures has recently been developed, with respect to the cable system elements only, less stresses in the bridge members or to control the vertical deflections of the deck, among others (Song, Xiao and Sun [17]; Lonetti and Pascuzzo [18]; Asgari, Osman and Adnan [19]; Cid, Baldomir and Hernández [20]).

In this paper, a Finite Element Method that employs a total Lagrangian position-based formulation, not based on displacement, was developed for application in static and dynamic analysis of simple cable structures. The Positional MEF was first approached in Coda [21]. Regarding the formulation for truss elements, that is the element used in this paper, one can also find several works, as seen in Greco et al. [22], Greco et al. [23], Carrazedo and Coda [24]; Greco and Ferreira [25]. Other research provides an interesting overview of different applications of the formulation: Fernandes, Coda and Sanches [26], Carrazedo, Paccola and Coda [27], Siqueira and Coda [28], Gomes and Beck [29], Soares, Paccola and Coda [30], Pascon and Coda [31] and Kan, Peng and Chen [32].

2 Formulation

This study uses an alternative formulation to solve the mechanical problem based on the Principle of the Minimum Mechanical Energy written regarding nodal positions. A brief review is made here mainly based on Coda [33], with current contributions in relation to the formulation so that the truss element can represent the cable element.

The total mechanical energy of a system is written in terms of potential energy of the applied forces ($\mathbb{P}$), total strain energy ($\mathbb{U}$) and kinetic energy ($\mathbb{K}$), as expressed:

$$\Pi = \mathbb{P} + \mathbb{U} + \mathbb{K} \ . \tag{1}$$

Therefore, to find the minimum energy one applies the first variation as:

$$\delta\Pi = \frac{\partial \Pi}{\partial \vec{Y}} \cdot \delta\vec{Y} = Grad\left(\Pi\right) \cdot \delta\vec{Y} = 0 \, , \tag{2}$$

in which the symbol δ means variation. Considering that the Eq. (2) is valid for any variation of the position, it is concluded that equilibrium occurs when

$$\frac{\partial \Pi}{\partial \vec{Y}} = \frac{\partial \mathbb{P}}{\partial \vec{Y}} + \frac{\partial \mathbb{U}}{\partial \vec{Y}} + \frac{\partial \mathbb{K}}{\partial \vec{Y}} = \vec{0} \, . \tag{3}$$

The potential energy of the applied forces can be written considering three force types: concentrated, distributed in parts of the surface ($\dot{q}$) or distributed in parts of the domain ($\vec{b}$), which, using index notation, results in:

$$\mathbb{P} = -F_i^{\alpha} Y_i^{\alpha} - \int_{S^{\beta}} q_i^{\beta}\left(S_0\right) y_i^{\beta}\left(S_0\right) dS_0 - \int_{\Omega^{\gamma}} b_i^{\gamma}\left(S_0\right) y_i^{\gamma}\left(\Omega_0\right) d\Omega_0 \, . \tag{4}$$

In Eq. (4), the terms Y_i^{α}, y_i^{β} or y_i^{γ} are the current position of the force, in which y are points of continuum and Y refers to isolated points; Ω_0 indicates domain and dS_0 is an infinitesimal area of the analyzed surface, and index 0 that the reference is the initial one (Lagrangian). As our problem is a simple truss element domain and surface forces are considered applied at nodes and the derivative of potential energy of the applied forces regarding the current position is given by:

$$\frac{\partial \mathbb{P}}{\partial Y_i} = -F_i \, . \tag{5}$$

The total strain energy can be written for the reference volume (V_0) or it can be understood as the work done by internal force (F^{int}), as:

$$\mathbb{U} = \int_{V_0} u_e dV_0 = \int_{Y_0}^{Y} F^{\text{int}}\left(Y\right) dY \, , \tag{6}$$

this implies that

$$\frac{\partial \mathbb{U}}{\partial \vec{Y}} = \vec{F}^{\text{int}} \, . \tag{7}$$

Without loss of generality, in the present study a linear elastic constitutive law relating second Piola-Kirchhoff stress (S) and Green strain ($\mathbb{E}$), usually called Saint-Venant-Kirchhoff elastic law was used for modeling the problem. For truss elements the uniaxial Green strain is given regarding length (ℓ) or current positions, as:

$$\mathbb{E} = \frac{1}{2}\frac{\ell^2 - \ell_0^2}{\ell_0^2} = \frac{1}{2}\left(\frac{\left(Y_1^2 - Y_1^1\right)^2 + \left(Y_2^2 - Y_2^1\right)^2 + \left(Y_3^2 - Y_3^1\right)^2}{\ell_0^2} - 1 \right) \, , \tag{8}$$

and the second Piola-Kirchhoff stress for Saint-Venant-Kirchhoff constitutive model is written as:

$$\frac{\partial u_e^{SVK}}{\partial \mathbb{E}} = \frac{\partial\left(\frac{K}{2}\mathbb{E}^2\right)}{\partial \mathbb{E}} = S^{SVK}\left(\mathbb{E}\right) = K\mathbb{E} \, . \tag{9}$$

in which K is the elastic constant that represents the Young modulus for small strains.

Further developing the Eq. (7), expanding by the chain rule and deriving the Eq. (8) one obtains the intern force:

$$F_i^{\text{int}} = \frac{\partial U_e}{\partial Y_k^\beta} = A_o \ell_0 \frac{\partial u_e(\mathbb{E})}{\partial \mathbb{E}} \frac{\partial \mathbb{E}}{\partial Y_k^\beta} = A_o \ell_0 S \frac{\partial \mathbb{E}}{\partial Y_k^\beta} = A_0 S \frac{(-1)^\beta}{\ell_0} \left(Y_k^2 - Y_k^1 \right). \tag{10}$$

Finally, it remains to determine the part of the energy that considers dynamic effects, called kinetic energy, as follows:

$$\mathbb{K} = \sum_{\alpha=1}^{mos} \mathbb{K}_\alpha = \frac{M_{(\alpha)} \dot{Y}_i^\alpha \dot{Y}_i^\alpha}{2}, \tag{11}$$

in which $\dot{Y}_i^\alpha$ is the velocity of the node α and ($M_{(\alpha)}$) is the mass associated with the node. By differentiating the Eq. (11) regarding current position, and doing some algebraic manipulations one can obtain:

$$\frac{\partial \mathbb{K}}{\partial Y_j^\gamma} = M_{(\alpha)} \ddot{Y}_i^\alpha = \frac{\rho A_0 \ell_0}{2} \ddot{Y}_i^\alpha = F_k^{inercial}, \tag{12}$$

where $\vec{F}^{inercial}$ is the inertial force, A_0 is the area, ρ is the mass density and $\ddot{\vec{Y}}_i^\alpha$ is the acceleration.

Thus, the dynamic equilibrium equation results in:

$$\vec{F}^{\text{int}} - \vec{F}^{ext} + \vec{F}^{iner} = \vec{0}. \tag{13}$$

2.1 Solution of nonlinear dynamic equilibrium equations

It can be noticed by the Eq. (10) that the internal forces are written in terms of the current position, which implies that the dynamic equilibrium equation is nonlinear regarding current positions. To solve the system of equations, the Newton-Raphson procedure is used by setting the unbalanced force vector ($\vec{g}$) in Eq. (13):

$$\vec{g} = \vec{F}^{\text{int}}\left(\vec{Y}\right) + \mathbf{M} \cdot \ddot{\vec{Y}} + \mathbf{C} \cdot \dot{\vec{Y}} - \vec{F}^{ext}\left(t\right) \tag{14}$$

where $\mathbf{C}$ is the damping matrix adopted proportional to the mass matrix ($\mathbf{C} = \lambda_c \cdot \mathbf{M}$). Equation (14) only returns zero when the exact equilibrium position is obtained.

The Newmark method, used for time integration, is summarized by the two following equations:

$$\vec{Y}_{s+1} = \vec{Y}_s + \dot{\vec{Y}}_s \Delta t + \left[\left(\frac{1}{2} - \beta \right) \ddot{\vec{Y}}_s + \beta \ddot{\vec{Y}}_{s+1} \right] \Delta t^2, \tag{15}$$

$$\dot{\vec{Y}}_{s+1} = \dot{\vec{Y}}_s + \left(1 - \gamma\right) \Delta t \ddot{\vec{Y}}_s + \gamma \Delta t \ddot{\vec{Y}}_{s+1}, \tag{16}$$

where β and γ are parameters of the method, assumed here to be 0.25 and 0.5, i.e., constant acceleration along time steps.

The Newton-Raphson method is applied by an expansion in Taylor series truncated in the first order of the Eq. (14), expressed as:

$$\vec{g}\left(\vec{Y}_{s+1}\right) = \vec{g}\left(\vec{Y}_{s+1}^0\right) + \nabla \vec{g}\left(\vec{Y}_{s+1}^0\right) \Delta \vec{Y} = \vec{0}, \tag{17}$$

where the $\vec{Y}_{s+1}^0$ is the trial position. From the Eq. (17) one obtains the Hessian matrix ($\mathbf{H}$):

$$\nabla \vec{g}\left(\vec{Y}_{s+1}\right) = \left. \frac{\partial^2 \Pi}{\partial \vec{Y}^2} \right|_{s+1} = \left. \frac{\partial^2 U_e}{\partial \vec{Y}^2} \right|_{s+1} + \frac{\mathbf{M}}{\beta \Delta t^2} + \frac{\gamma \mathbf{C}}{\beta \Delta t} = \mathbf{H}^{static} + \frac{\mathbf{M}}{\beta \Delta t^2} + \frac{\gamma \mathbf{C}}{\beta \Delta t} = \mathbf{H}, \tag{18}$$

and calculates the position correction:

$$\Delta\vec{Y} = -\mathbf{H}^{-1} \cdot \vec{g}\left(\vec{Y}_{s+1}^{0}\right). \tag{19}$$

Thus, the $\Delta\vec{Y}$ is used to calculate a new trial position, as

$$\vec{Y}_{s+1}^{0} = \vec{Y}_{s+1}^{0} + \Delta\vec{Y}, \tag{20}$$

and therefore velocity and acceleration, see Eq. (15) and Eq. (16).

The stop criterion considers a chosen tolerance (*tol*) and is given by

$$\frac{|\Delta Y_k|}{|X_k|} \leq tol. \tag{21}$$

It remains to determine the static Hessian matrix $\mathbf{H}^{static}$, by developing the corresponding term from Eq. (18) and using the properties of the Kronecker delta (δ_{ij}) and other simple algebraic manipulations, results

$$\left.\frac{\partial^2 U_e}{\partial Y_k \partial Y_i}\right|_{\vec{Y}^0} = \left(H_{ik}^{\alpha\beta}\right)_{static}^{j} = (-1)^{\beta}(-1)^{\alpha}\frac{A_0^{(j)}}{\ell_0}\left(K\frac{\left(Y_i^2 - Y_i^1\right)}{\ell_0}\frac{\left(Y_k^2 - Y_k^1\right)}{\ell_0} + S\delta_{ik}\right). \tag{22}$$

The algorithm presented can be used both for the static problem and for the dynamic problem, by simply changing the characteristic input data of the dynamic problem: mass density, Newmark parameters and increment of time, in order to disregard the part of kinectic energy ($\mathbb{K}$) related to the dynamic effects.

2.2 Active Elements

In order to simulate the pretension of cables or even actuators present in movable structures (or mechanisms), it is proposed to use the truss element described above as active elements or uniaxial actuators. The actuators are truss elements subjected to a shortening or lengthening. This is done by rewriting Eq. (8) as

$$\mathbb{E} = \frac{1}{2}\frac{\ell^2 - \left(\ell_0 + \Delta\ell_e\right)^2}{\ell_0^{\,2}}, \tag{23}$$

in which $\Delta\ell_e$ is the change of length imposed to each element, written in terms of the current time (t_{s+1}), as follows:

$$\Delta\ell_e = a + b \cdot t_{s+1} + c \cdot t_{s+1}^2 + d \cdot sen\left(e \cdot t_{s+1}\right), \tag{24}$$

where a , b , c and d are constants.

2.3 Providing continuous forces on cables

A continuous cable has continuity of forces along its length, therefore this strategy is intended to adjust forces in the cables in order to provide its continuity for different spans of suspension bridges or tension structures, or even, simply impose equal forces between disconnected cables. From Eq. (9) and supposing, for simplification, a linear strain, the change value of the length to be imposed on the cable elements is given by:

$$\Delta\ell_a = \frac{|A_1 S_1 - A_2 S_2|}{K\left(A_1 + A_2\right)/2} \cdot \ell_0, \tag{25}$$

in which S_1 and S_2 is the stress in the cables analyzed and A_1 and A_2 are their areas. The $\Delta\ell_a$ is added to the value of $\Delta\ell_a$, in Eq. (24). The process continues until the following convergence condition is satisfied:

$$\frac{|F_1 - F_2|}{\left(|F_1 + F_2|/2\right)} \leq tol\,, \tag{26}$$

in which F_1 and F_2 are the cables forces.

In suspension bridges, the continuity of cables can be made even more accurate, by simulating the saddle at the top of the bridge towers, as briefly described in the next section.

2.4 Simple penalty technique to simulate sliding saddles and pulleys

The truss element is also used to simulate continuous cables over saddles and / or pulleys. in order to make it possible, a limit length for special elements (penalty) and the point of rotation are defined. Special elements have zero modulus of elasticity when their lengths are greater than the predefined length (inactive element) and assume high modulus of elasticity when lengths tends to be less than the predefined one (active element). An active element is deactivated when it presents positive stress values. As it is a trivial penalty technique, to save space, no further details will be given in this paper.

2.5 Removal of numerical singularity of cable problems

For the regularization of the Hessian matrix in statically cable problems different techniques can be used, in this paper three alternatives were evaluated: (i) pretension and special boundary conditions; (ii) damped dynamic analysis and (iii) modified dynamic analysis. In this third technique, the mass matrix is added in the Hessian matrix, but its influence is reduced at each Newton-Raphson iteration as:

$$\mathbf{H} = \mathbf{H}^{static} + \frac{\mathbf{M}}{\beta \Delta t^2} \cdot \frac{1}{st} \tag{27}$$

in which st is the iteration number. Therefore, the last iteration of each load step is done using static model, for the refinement of the equilibrium position of the structure. Moreover, no inertial force is considered.

3 Numerical Examples

Six examples are selected to verify and to present the applications of the formulation. The tolerance adopted for equilibrium verification is $tol = 1 \times 10^{-14}$.

3.1 Crane

The following example is taken from Baiocco [34] and is used to validate the developed code regarding loading phases. It is a crane, which the spear is lifted by the action of an actuator located at the top end of the tower. At the end of the spear a static load of $F = 3.2\,kN$ is applied in the vertical direction and downward. The actuator is shortened until the final length of 180 *mm* is reached, considering an initial length of $165\sqrt{2} \approx 233.34\,mm$. A lengthening of equal value is also applied so that the spear moves downwards. The structure was moved in four phases, corresponding to: raising the spear, lowering to the initial position, lowering until the lengthening imposed on the actuator element is reached and, finally, returning the spear to the initial position. The actuator length change, in each phase, was imposed in 15 steps.

The crane bars have 45 *mm* diameter circular cross section and the material has an elastic modulus 210 *GPa*. The adopted boundary conditions and steel bars elements are displayed in Fig. 1.

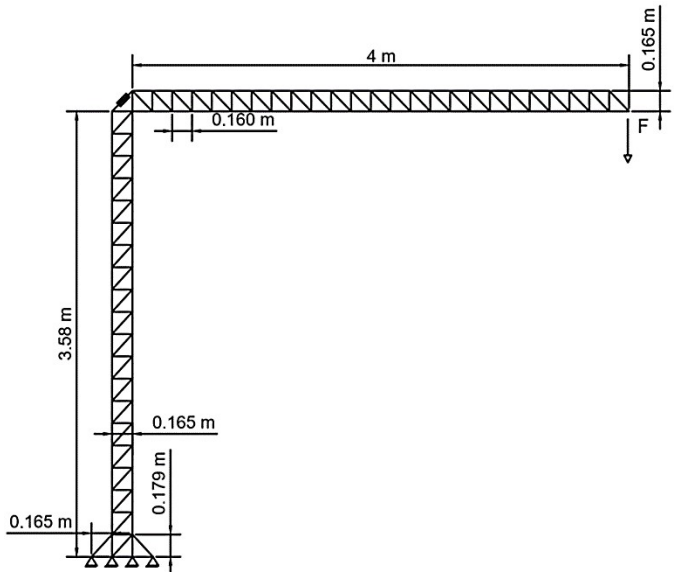

Figure 1. Simulated crane with actuator element

Figure 2 shows the displacement of the crane spear at the end of the first and third phases, as well as the normal forces on the elements after upward movement of the spear.

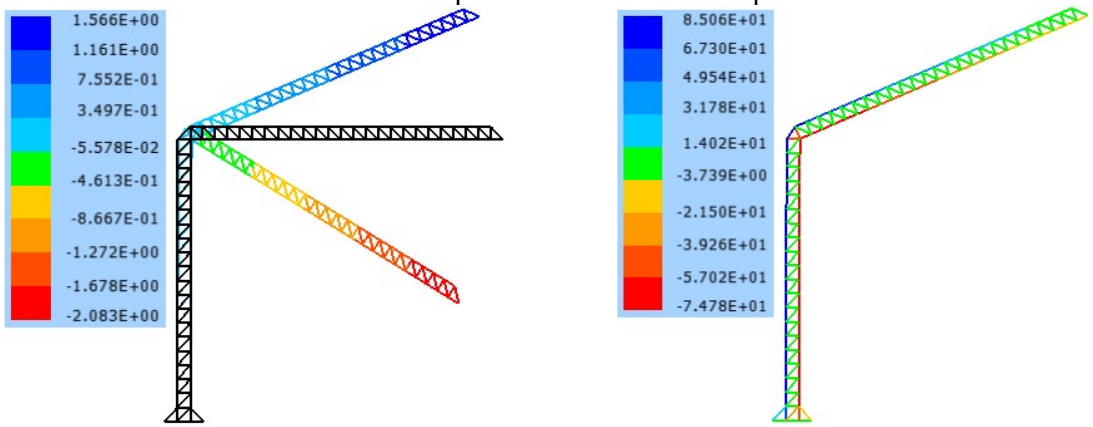

(a) Vertical displacement (*m*) **(b) Normal force in the elements (*kN*)**

Figure 2. Vertical displacement and normal force on the crane

3.2 Cable subjected to a uniform distributed load

The problem is solved here using the proposed numerical model and compared with the parabolic analytical solution (Schiel [35]). We adopt a distributed load (p) of 2 *kN/m*, the length of the cable of 10 meters and an arrow (f) of one meter. From these values it is possible to calculate the geometrical parameters of the cable, as well as the internal force. The cable model is given in Fig. 3.

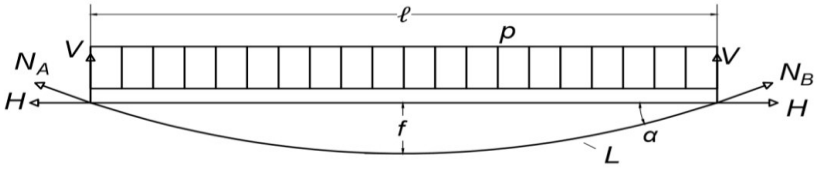

Figure 3. Parabolic cable: Adapted from Schiel [35]

Calculating the inclination (ϕ), the horizontal (H) and vertical (V) force at the ends of the cable, one can obtain the normal force (N) in the cable and the final length (L) of the cable, as given

by

$$\phi = tg\,\alpha = \frac{4f}{\ell} = 0.40\,, \tag{28}$$

$$V = \frac{p\ell}{2} = 10kN\,, \tag{29}$$

$$H = \frac{p\ell^2}{8f} = 25\,kN\,, \tag{30}$$

$$N_A = N_B = N = \sqrt{V^2 + H^2} \approx 26.93\,kN\,, \tag{31}$$

$$L = \ell \cdot \lambda = \ell \cdot \left[\frac{1}{2}\sqrt{1+\phi^2} + \frac{1}{2\phi}\ln\left(\phi + \sqrt{1+\phi^2}\right)\right] \approx 10.26\,m\,. \tag{32}$$

The same problem is solved using the developed computational code and three models were used as a way to regularize the analysis of cable problems: by means of pretension, by dynamic problem and using the modified dynamic technique.

The first regularization scheme is divided in four phases, depicted in Fig. 4. In the first one, the structure is simulated statically by applying a shortening of 1% in the length of each bar element, providing roller supports in the intermediate nodes so that the structure does not present singular Hessian. In the second phase, the reduction of the elements is maintained, which would be equivalent to a pretension and then the roller supports can be removed, since the Hessian will not be more singular, as well the distributed load can be applied. In the third phase, the elements are lengthened until they return to the initial length (ℓ). Finally, in the last phase, the elements are lengthened until reaching the final length (L) calculated by means of the Eq. (32). The first three phases were performed in 10 steps, and the fourth phase in 26 steps.

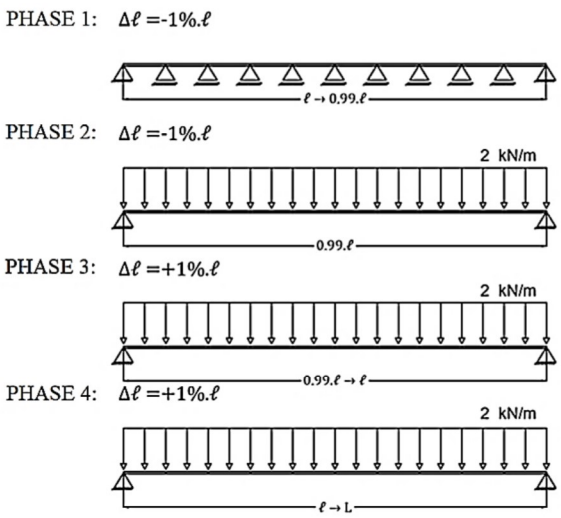

Figure 4. Cable submitted to distributed load resolved by static model

The second regularization scheme is solved in two phases. In the first phase, the distributed load was applied dynamically in 500 steps of time. In addition, a mass density of 7000 kg / m^3 and a mass proportional damping coefficient of 0.5 were considered. In the second phase, the cable was statically simulated, with the elements lengthened at 1% of the length until the calculated final length (L) was reached. For this, 26 steps were required.

The last regularization scheme is solved using the modified dynamic model. In the first phase the load was applied in 10 steps of fictitious time with the modified Hessian matrix and another step using static model, and after the cable was lengthened in 26 steps until reaching the previously calculated

length (L), also using static model.

The cable diameter is 2 *cm* and the material used is steel, assuming an elastic modulus of 210 *GPa*.

In order to evaluate the influence of the discretization on the accuracy of results, two discretization were adopted: one with ten finite elements ($\Delta\ell_{10}$) and the other with twenty finite elements ($\Delta\ell_{20}$).

In Fig. 5, the vertical displacement for the two discretization are presented. It is observed that the value of the obtained arrow was very close to the value used in the analytical model (1 *m*).

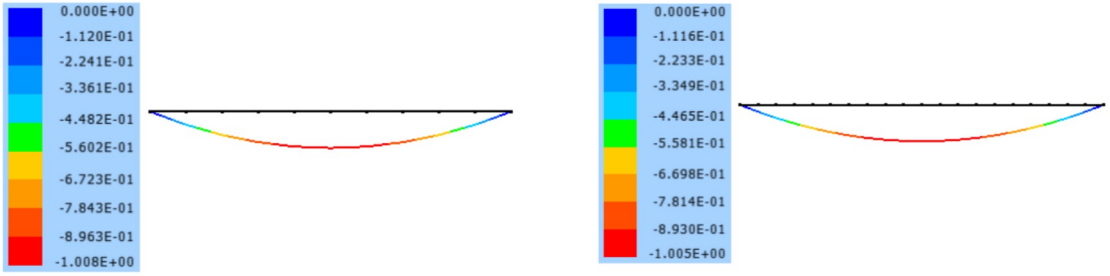

(a) 10 elements (b) 20 elements

Figure 5. Vertical displacement, in meters (*m*)

At the last step, the normal forces values are the ones depicted in Fig. 6. The force value at the end of the cable calculated using the present formulation ($N_{\Delta\ell_{10}} = 26.07\ kN$ and $N_{\Delta\ell_{20}} = 26.33\ kN$) and using the analytical model ($N = 26.93\ kN$) are very close.

The results obtained by means of the three regularization schemes are identical, thus, Fig. 5 and Fig. 6 correspond to the results found by the three simulation strategies used. The modified dynamic model dispenses some phases, necessary in the technique of the static model, and this is the model that presents better convergence.

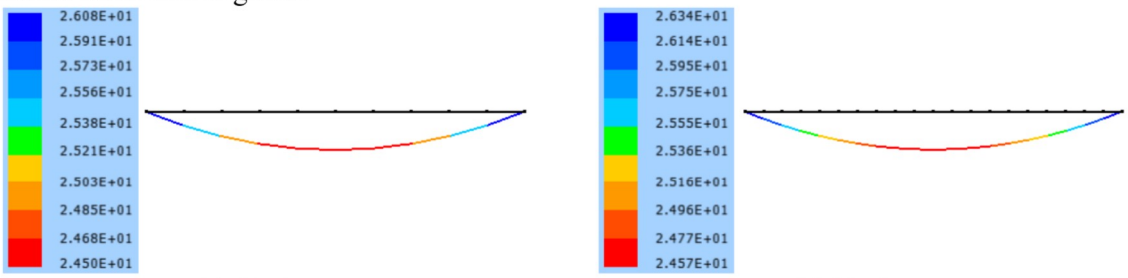

(a) 10 elements (b) 20 elements

Figure 6. Normal force on the cable in the last step (*kN*)

In this way, we conclude that the positional based truss finite element is capable of representing cable structures. In addition, it turns out that 10 finite elements are sufficient to statically simulate cables with good accuracy.

3.3 Three-dimensional Tension Structure

This example, although simple, already brings the basic idea of the behavior of a tension structure, and mainly, closer to a tensegric shell system. It is a structure composed of cables that must work under tension, whose diameter is 1 *cm*, and vertical bars, which should be compressed, with 10 *cm* diameter. Figure 7 shows the geometry of the structure and the applied load.

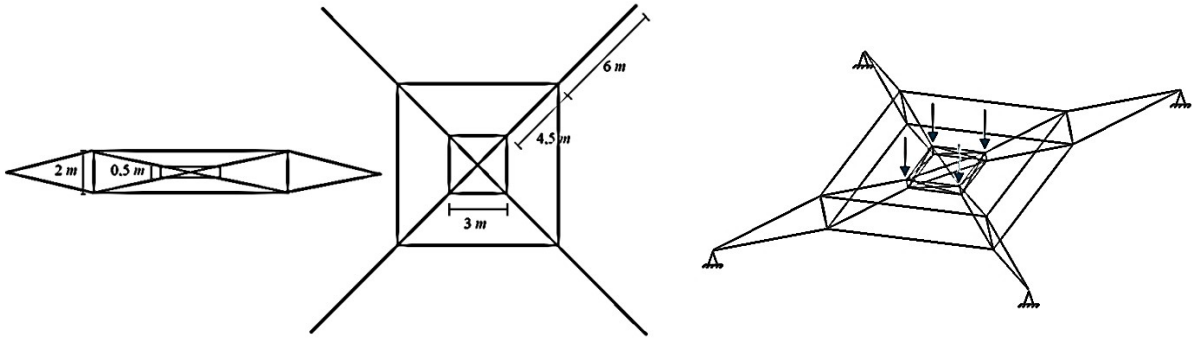

Figure 7. Geometry of the tension structure

The problem was solved in two phases. Initially, the vertical bars, which are the actuators elements, are lengthened in 1% of the length, and in this way the cables are subjected to a tension. Then, the load ($F = 5\,kN$) can be applied to the structure without loss of stability, because the cables remain tensioned. In fact, in this case, there was only a tension relief in the upper cables. The material has an elastic modulus of 210 *GPa*.

It can be observed that the structure already has an initial instability, due to the presence of intermediate nodes in the cables. However, as the cables are all tensioned, the structure does not lose stability and even can be solved using static model.

The normal forces in the elements of the structure and the nodes position can be seen in Fig. 8.

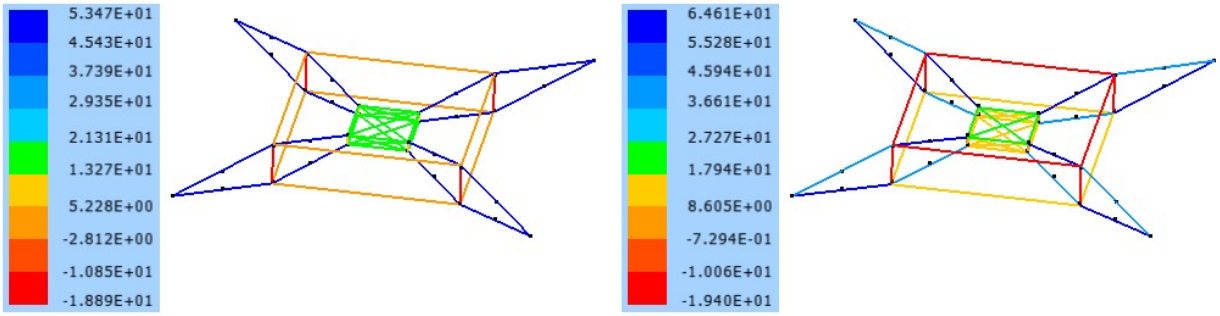

(a) After lengthen of the actuator **(b) After load application**

Figure 8. Normal forces on tension structure (*kN*)

3.4 Cable force continuity

A cable subjected to two different concentrated loads in each side ($F_1 = 5\,kN$ and $F_2 = 10\,kN$) is analyzed to show the proposed strategy to simulate continuous force in cables gives good results. The material properties are: circular cross section with diameter of 10 *mm*, Young modulus equal to 210 *GPa* e mass density of 7000 *kg/m³*. A sketch is given in Fig. 9.

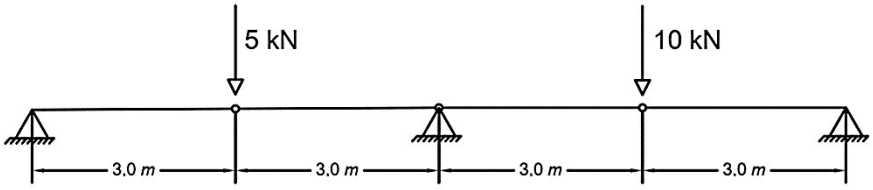

Figure 9. Four cables subjected to different forces in each span

In the first phase the load was applied in 10 steps without matching cable force, using modified dynamic technique. In the second phase the force of the two central cables was matched, using static model. The normal forces in the cable are presented in the Fig. 10 and the horizontal displacement

after matching forces is given in Fig. 11.

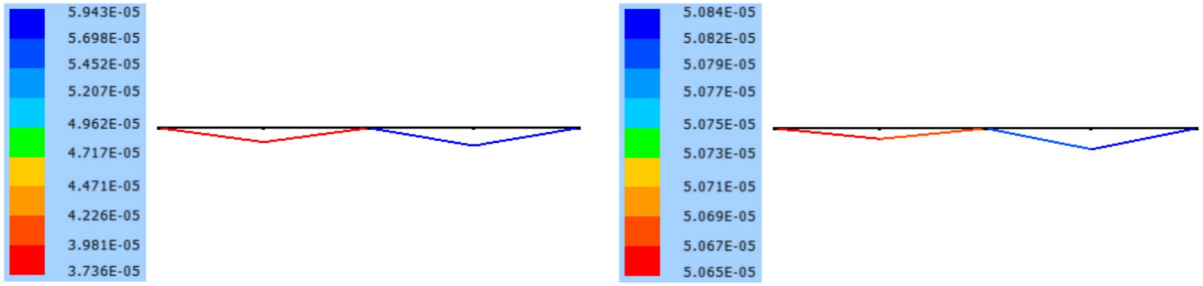

(a) Before imposing equal forces (b) After imposing equal forces

Figure 10. Normal force on cables ($\times 10^6\ kN$)

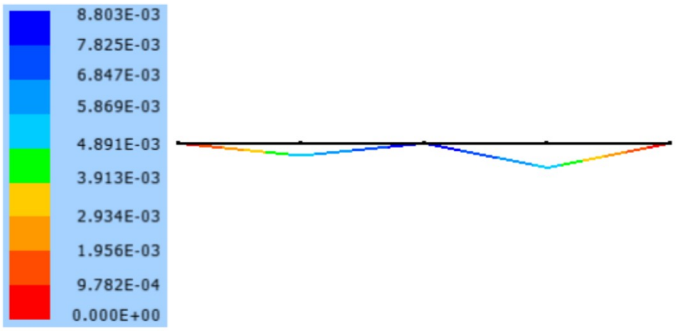

Figure 11. Horizontal displacement due to force adjustment (m)

3.5 Pulley

This example is a three-dimensional model of a pulley with a cable subject to self-weight. The pulley is modeled by special penalty truss elements. The problem was simulated in two phases: one of load application and another for the movement of the cable through the pulley, by lengthening ($\Delta\ell = 1cm$) the cable near the lower support (Fig. 12).

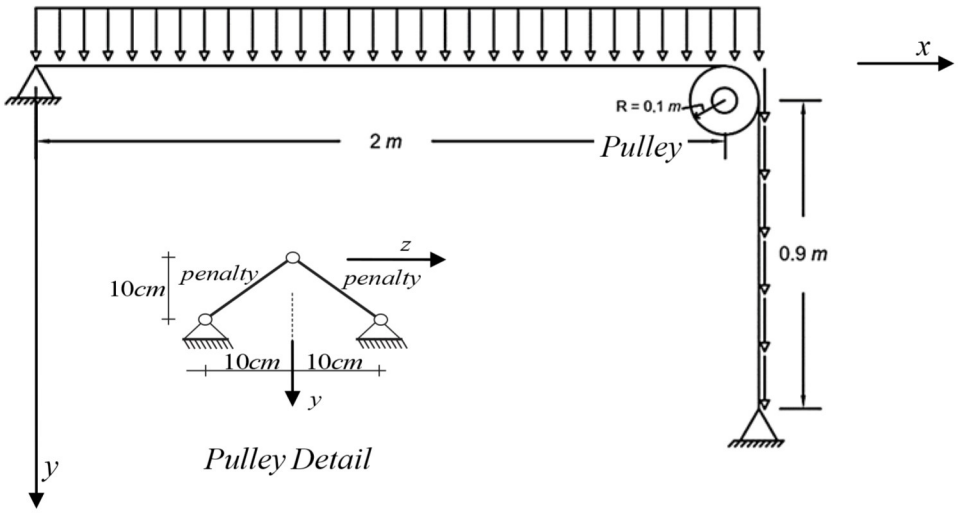

Figure 12. Geometry of a pulley - 3D

The cable has a diameter of 10 mm, elastic modulus of 210 GPa and mass density equal to 7000 kg/m^3, thus the load corresponding to the self-weight is of $5{,}5\times10^{-3}\ kN/m$. Each phase was modelled using 100 steps, in which the first one used a dynamic model with a mass proportional

damping coefficient equal to 0.05 and in the second phase the modified dynamic model was used, considering an auxiliary mass matrix and a pseudo time step equal to the real one.

Figure 13 shows the vertical displacement in the first and second phase without showing special elements (penalty). Figure 14 shows the normal force in the cable after lengthening of the element, see that special elements are displayed in perspective. It can be noticed in Fig. 12 that, because it is a three-dimensional model, the pulley is simulated by means of two elements that connect pinned supports to each node which has the possibility of having the restricted displacement, in other words, pass through the pulley. The distance between the pinned supports corresponds to the width of the pulley.

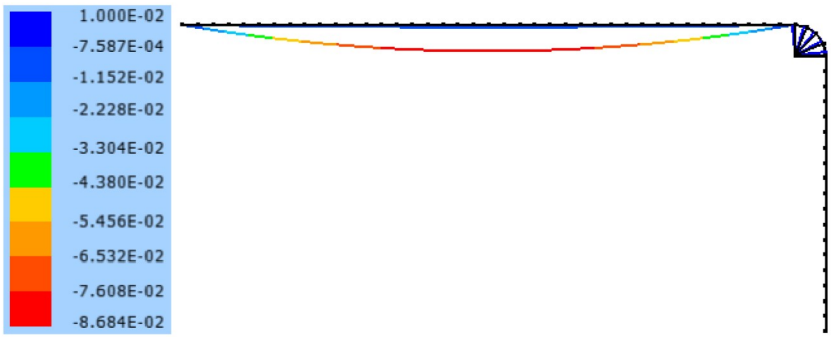

Figure 13. Vertical displacement of the cable in the pulley (m)

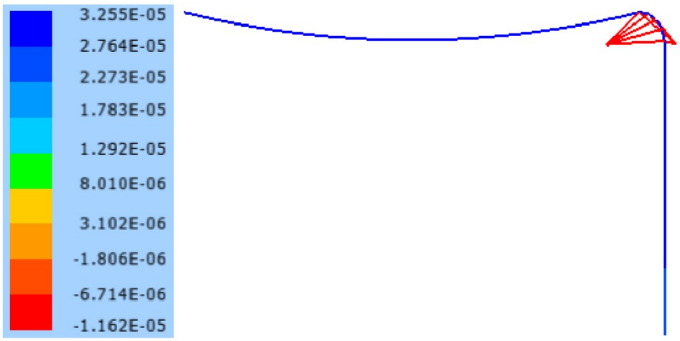

Figure 14. Normal force on cable in the pulley ($\times 10^3\ kN$)

3.6 Bascule Bridge

A moveable bridge is simulated using an actuator to move the bridge and a special element (penalty) to simulate the central column, three phases are modelled. First, in order to lift the bridge, the cable is shortened ($\Delta\ell = -30\,cm$), and the element corresponding to the column, that is the special element in this case, remains deactivated. Then the cable is lengthened to its initial length and the bridge return to the horizontal position. Therefore, the column reaches its initial length, meaning that it is activated and comes to support the bridge. The analyzed bascule bridge is shown in Fig. 15.

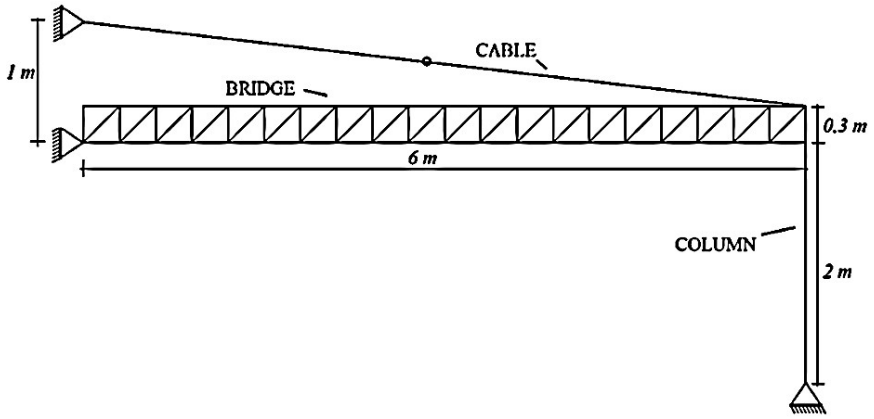

Figure 15. Geometry of a moveable bridge

The material properties assumed for this analysis are: diameter of the cable $d_c = 10\,mm$, cross-section area of the horizontal truss bars $A_h = 50\,cm^2$ and of vertical and diagonal bars are $A_{vd} = 81.2\,cm^2$, $E = 210\,GPa$ and $\rho = 7000\,kg/m^3$. During the lifting of the bridge, a distributed load of 2 *kN/m* is applied on the structure and when in horizontal position the value of distributed load is 10 *kN/m*.

The vertical displacement in the first phase is illustrated in Fig. 16 and see that the special element (column) is not shown.

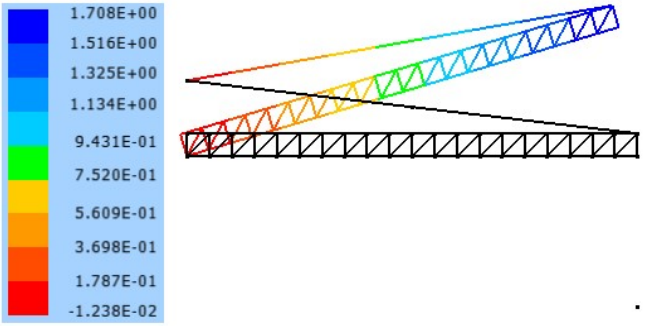

Figure 16. Vertical displacement at the final of the first phase

The normal force in the structure is presented in Fig. 17. It can be observed that during lifting the bridge, the (special) column element has zero normal force and when the bridge is in the horizontal position, with a distributed load, the column is compressed and the cable has zero normal force on it.

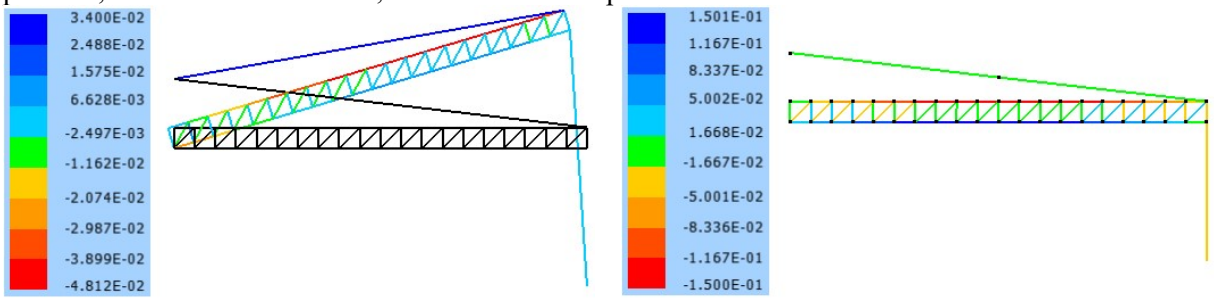

(a) First phase **(b) Third phase**

Figure 17. Normal force on the moveable bridge

4 Conclusions

An alternative formulation of the Finite Element Method, based on nodal positions, for static and

dynamic analysis has been proposed and successfully implemented for the analyses of tension structures and cables. Using space truss elements adapted to simulate positional actuators the present formulation is capable of simulate pretensioned cables and compressive actuators, which are of practical interest. Three techniques to remove the numerical singularity of statically cable problems were used, concluding that the modified dynamic model was the one that presented better convergence and simpler use. The formulation is also adapted to simulate restriction of displacement problems (penalty) and to provide equal forces on chosen cables in a simplified way. Six examples were shown demonstrating the accuracy, stability and applicability of the formulation. Future developments include the extension of the proposed formulation to simulate representative models of suspension bridges, cable-stayed bridges and cable roof structures, and to analyze vibration and transient problems in near unstable structures.

Acknowledgements

Authors would like to thanks CAPES (Coordenação de Aperfeiçoamento de Pessoal de Nível Superior) for the financial support of this research (Finance Code 001).

References

[1] K. Santoso. Wide-Span Cable Structures. Master's thesis, Massachusettes Institude of Technology, 2004.
[2] H. A. Buchholdt. *An introduction to cable roof structures.* Press Syndicate of the University of Cambridge, 1999.
[3] L. Jia; C. Zhag; Y. Jiang; J. Cheng; R. Xiao. Simplified Calculation Methods for Static Behaviors of Triple-Tower Suspension Bridges and Parametric Study. *International Journal of Steel Structures*, vol. 18, n. 2, pp. 685–698, 2018.
[4] M. R. Jung; D. J. Min; M. Y. Kim. Simplified analytical method for optimized initial shape analysis of self-anchored suspension bridges and its verification. *Mathematical Problems in Engineering*, vol. 2015, 2015.
[5] X. Wang; S. Chai; Y. Xu. Deformation Characteristics of Double-Cable Multispan Suspension Bridges. *Journal of Bridge Engineering*, vol. 21, n. 4, pp. 1–8, 2016.
[6] W. M. Zhang.; L. Shi; L. Li; Z. Liu. Methods to correct unstrained hanger lengths and cable clamps' installation positions in suspension bridges. *Engineering Structures*, vol. 171, pp. 202–213, 2018.
[7] D. W. Chen; F. T. K. Au; L. G. Tham; P. K. K. Lee. Determination of initial cable forces in prestressed concrete cable-stayed bridges for given design deck profiles using the force equilibrium method. *Computers and Structures*, vol. 74, n. 1, pp. 1–9, 2000.
[8] A. L. H. de C. El Debs. Determinação de Coeficiente de Impacto em Pontes Estaiadas sob a Ação de Cargas Móveis. PhD thesis, School of Engineering of São Carlos, University of São Paulo, 1990.
[9] M. N. Chatzis; G. Deodatis. Modeling of Very Large Interacting Multiple-Beam Systems with Application to Suspension Bridge Cables. *Journal of Structural Engineering*, vol. 139, n. 9, pp. 1541–1554, 2013.
[10] C. A. M. Filho. Análise estática não linear plana de pontes estaiadas e determinação das frequências naturais e modos de vibração. Master's thesis, School of Engineering of São Carlos, University of São Paulo, 2014.
[11] D. Feng; C. Mauch; S. Summerville; O. Fernandez. Suspender Replacement for a Signature Bridge : a Case Study Suspender Replacement for a Signature Bridge. *Journal of Bridge Engineering*, vol. 23, pp. 1–10, 2018.
[12] H. K. Kim; M. J. Lee; S. P. Chang. Non-linear shape-finding analysis of a self-anchored suspension bridge. *Engineering Structures*, vol. 24, n. 12, pp. 1547–1559, 2002.
[13] A. M. L. Cardoso. Estudo da Rigidez Efetiva do Cabo de Ponte Estaiadas. Master's thesis, School of Engineering of São Carlos, University of São Paulo, 2013.

[14] M. F. Q. Ytza. Métodos Construtivos de Pontes Estaiadas - Estudo da Distribuição de Forças nos Estais. Master's thesis, University of São Paulo, 2009.
[15] Z. R. Feng; J. Shen; X. J. Wang. Finite Element Analysis of Thermal Stress for Cable-Stayed Bridge Tower with Cracks. *Applied Mechanics and Materials*, vol. 178–181, pp. 2085–2090, 2012.
[16] D. Yang; T. Yi; H. Li; Y Zhang. Correlation-Based Estimation Method for Cable-Stayed Bridge Girder Deflection Variability under Thermal Action. v. 32, n. 2016, p. 1–10, 2018.
[17] C. Song; R. Xiao; B. Sun. Optimization of cable pre-tension forces in long-span cable-stayed bridges considering the counterweight. *Engineering Structures*, vol. 172, pp. 919–928, 2018.
[18] P. Lonetti and A. Pascuzzo. Optimum design analysis of hybrid cable-stayed suspension bridges. *Advances in Engineering Software*, vol. 73, pp. 53–66, 2014.
[19] B. Asgari; S. A. Osman; A. B. Adnan. Optimization of Pre-Tensioning Cable Forces in Highly Redundant Cable-Stayed Bridges. *International Journal of Structural Stability and Dynamics*, vol. 15, n. 1, pp. 1–16, 2015.
[20] C. Cid; A. Baldomir; S. Hernández. Optimum crossing cable system in multi-span cable-stayed bridges. *Engineering Structures*, vol. 160, pp. 342–355, 2018.
[21] H. B. Coda, 2003. An exact FEM geometric non-linear analysis of frames based on position description. In: São Paulo, *17th International Congress of Mechanical Engineering (COBEM 2003)*.
[22] M. Greco; F. A. R. Gesualdo; W. S. Venturini; H. B. Coda. Nonlinear positional formulation for space truss analysis. *Finite Elements in Analysis and Design*, vol. 42, n. 12, pp. 1079–1086, 2006.
[23] M. Greco; R. C. G. Menin; I. P. Ferreira; F. B. Barros. Comparison between two geometrical nonlinear methods for truss analyses. *Structural Engineering and Mechanics*, vol. 41, n. 6, pp.735-750, 2012.
[24] R. Carrazedo and H. B. Coda. Alternative positional FEM applied to thermomechanical impact of truss structures. *Finite Elements in Analysis and Design*, vol. 46, n. 11, pp. 1008–1016, 2010.
[25] M. Greco and I. P. Ferreira. Logarithmic strain measure applied to the nonlinear positional formulation for space truss analysis. *Finite Elements in Analysis and Design*, vol. 45, n. 10, pp. 632–639, 2009.
[26] J. W. D. Fernandes; H. B. Coda; R. A. K. Sanches. ALE incompressible fluid – shell coupling based on a higher-order auxiliary mesh and positional shell finite element. *Computational Mechanics*, vol. 63, n. 3, pp. 555–569, 2019.
[27] R. Carrazedo; R. R. Paccola; H. B. Coda. Active face prismatic positional fi nite element for linear and geometrically nonlinear analysis of honeycomb sandwich plates and shells. *Composite Structures*, vol. 200, pp. 849–863, 2018.
[28] T. M. Siqueira and H. B. Coda. Total Lagrangian FEM formulation for nonlinear dynamics of sliding connections in viscoelastic plane structures and mechanisms. *Finite Elements in Analysis and Design*, vol. 129, pp. 63–77, 2017.
[29] W. J. de S. Gomes and A. T. Beck. Global structural optimization considering expected consequences of failure and using ANN surrogates. *Computers and Structures*, vol. 126, pp. 56–68, 2013.
[30] H. B. Soares; R. R. Paccola; H. B. Coda. Unconstrained Vector Positional Shell FEM formulation applied to thin-walled members instability analysis. *Thin-Walled Structures*, vol. 136, pp. 246–257, 2019.
[31] J. P. Pascon and H. B. Coda. A shell finite element formulation to analyze highly deformable rubber-like materials. *Latin American Journal of Solids and Structures*, vol. 10, pp. 1177–1209, 2013.
[32] Z. Kan; H. Peng; B. Chen. Complementarity Framework for Nonlinear Analysis of Tensegrity Structures with Slack Cables. *AIAA Journal*, vol. 56, n. 12, 2018.
[33] H. B. Coda. *O Método Dos Elementos Finitos posicional: Sólidos e Estruturas - Não linearidade Geométrica e Dinâmica*. São Carlos: EESC-USP, 2018.
[34] M. H. Baiocco. Uma Iniciação à Mecânica dos Sólidos Não Linear com Aplicações à Biomecânica via Método dos Elementos Finitos. FAPESP Report, School of Engineering of São Carlos, University of São Paulo, 2012.
[35] F. Schiel. *Introdução à Resistência de Materiais*. Harbra, 1984.